Author Manuscript

Author Manuscript

Author Manuscript

Author Manuscript

HHS Public Access

Author manuscript

J Bone Miner Res. Author manuscript; available in PMC 2016 January 28.

Published in final edited form as:

J Bone Miner Res. 2015 February ; 30(2): 309–317. doi:10.1002/jbmr.2327.

PTH Receptor Signaling in Osteoblasts Regulates Endochondral Vascularization in Maintenance of Postnatal Growth Plate

Tao Qiu[1], **Lingling Xian**[1], **Janet Crane**[1], **Chunyi Wen**[2], **Matthew Hilton**[3], **William Lu**[2], **Peter Newman**[4], and **Xu Cao**[1]

[1]Department of Orthopaedic Surgery, Johns Hopkins University School of Medicine, Baltimore, MD, USA

[2]Department of Orthopaedics and Traumatology, University of Hong Kong, Hong Kong, China

[3]Department of Orthopaedics and Rehabilitation, University of Rochester School of Medicine, Rochester, NY, USA

[4]Blood Research Institute, Blood Center of Wisconsin, Milwaukee, WI, USA

Abstract

Longitudinal growth of postnatal bone requires precise control of growth plate cartilage chondrocytes and subsequent osteogenesis and bone formation. Little is known about the role of angiogenesis and bone remodeling in maintenance of cartilaginous growth plate. Parathyroid hormone (PTH) stimulates bone remodeling by activating PTH receptor (PTH1R). Mice with conditional deletion of PTH1R in osteoblasts showed disrupted trabecular bone formation. The mice also exhibited postnatal growth retardation with profound defects in growth plate cartilage, ascribable predominantly to a decrease in number of hypertrophic chondrocytes, resulting in premature fusion of the growth plate and shortened long bones. Further characterization of hypertrophic zone and primary spongiosa revealed that endochondral angiogenesis and vascular invasion of the cartilage were impaired, which was associated with aberrant chondrocyte maturation and cartilage development. These studies reveal that PTH1R signaling in osteoblasts regulates cartilaginous growth plate for postnatal growth of bone.

Keywords

PARATHYROID HORMONE; VASCULARIZATION; POSTNATAL BONE GROWTH; GROWTH PLATE

Introduction

Parathyroid hormone (PTH) is a systemic hormone that is known to regulate calcium homeostasis and bone remodeling. Evolutionarily, the parathyroid glands emerged in amphibians when vertebrate animals came to land, allowing mobilization of calcium where

Address correspondence to: Tao Qiu, PhD, or Xu Cao, PhD, Department of Orthopaedic Surgery, Johns Hopkins University School of Medicine, 720 Rutland Avenue, Ross 229, Baltimore, MD 21205, USA. tqiu4@jhmi.edu or xcao11@jhmi.edu.

Disclosures All authors state that they have no conflicts of interest.

Author Manuscript Author Manuscript Author Manuscript Author Manuscript

dietary sources were less available. Additionally, other modifications to the skeleton were essential for mobilization on land, including the growth of limbs. Previous studies have implicated that PTH plays a role in this process. The action of PTH is evidenced in the frog, *X. laevis*, where the PTH receptor becomes expressed at the same time the frog begins growing limbs.[1] In mammals, similarly, parathyroid glands are developed at the late embryonic stage when limbs begin to develop.[2] Limb growth occurs through endochondral ossification, which depends on a first-formed cartilage mold, invasion of blood vessels, and subsequent bone replacement. This process proceeds outward and establishes two growth plates on primary trabeculae that separate the distal cartilaginous epiphyses from the medial bony diaphysis. The elongation of bone is determined by an incremental shift of growth plate cartilage away from the diaphysis through intricate autocrine, paracrine, and endocrine hormone signaling pathways.

Further evidence suggests that PTH promotes longitudinal bone growth. In PTH knockout mice, the length of bone tissue was reduced and the cartilage matrix mineralization was diminished.[3] When PTH levels are suppressed by diet-induced hypophosphatemia/hypercalcemia, animals exhibited shortened limbs in addition to a ricket-like bone phenotyp.[4] PTH mediates intracellular signaling by binding to the G-protein coupled type 1 PTH receptor (PTH1R) and activating adenylate cyclase.

Clinically, inactivating mutations in PTH1R lead to Blomstrand's lethal chondrodysplasia,[5] whereas activating mutations lead to Jansen's metaphyseal chondrodysplasia.[6] Both are characterized by shortened limbs and abnormal bone mineralization. Additionally, inactivating mutations in Gαs lead to Albright's hereditary osteodystrophy, a disorder characterized by a lack of responsiveness to PTH and short stature from premature closure of the growth plate.[7,8] These observations suggest a role of PTH in cartilage development and longitudinal growth of bone.

PTH exerts its anabolic effect on bone partly through orchestrating signaling of local factors including TGFβ, Wnts, BMP, and IGF-1.[9–13] Importantly, PTH is able to improve bone marrow microenvironment. For example, intermittent injection of PTH spatially relocates blood vessels closer to sites of new bone formation to facilitate bone remodeling,[14] and expands both hematopoietic stem cells (HSC) and mesenchymal stem cells (MSC).[15,16] It is of interest to know whether the PTH-induced changes in bone marrow microenvironment have potential effects on growth plate cartilage.

In contrast to extensive studies performed on the role of cartilage in regulation of osteogenesis and bone formation, little is known about whether angiogenesis and bone remodeling regulate chondrocytes. Herein, we found that mice with deletion of PTH1R in osteoblasts have disrupted trabecular bone formation. Interestingly, the mice were also noted with a reduction in vascular invasion of cartilage and growth plate abnormalities with a decrease of hypertrophic chondrocytes. This phenotype is distinct from the accelerated chondrocyte differentiation observed previously in mice with chondrocyte-specific deletion of PTH1R.[4,17–19] Therefore, our data reveal that PTH receptor signaling in osteoblasts regulates postnatal growth plate.

Author Manuscript Author Manuscript Author Manuscript Author Manuscript

Materials and Methods

Mice

Mice with osteoblast-specific deletion of (*PTH1R*$^{-/-}$) were generated by crossing mice homozygous for a floxed PTH1R allele[20] with Cre-transgenic mice driven by a 4-kb human osteocalcin promoter (OC-Cre mice).[21] Mice with osteoblast-specific inactivation of TβRII (*TβRII*$^{-/-}$) were generated by crossing the OC-Cre mice with mice homozygous for a floxed TβRII allele.[9] Knockout mice with homozygous for PECAM-1 allele were created by self-crossing the heterozygous mice from Dr. Peter Newman.[22,23] All procedures involving animals were maintained in the Animal Facility of Johns Hopkins University School of Medicine. The animal protocols were reviewed and approved by the Institutional Animal Care and Use Committee of the Johns Hopkins University (Baltimore, MD, USA).

Histology, immunohistochemistry, and in situ hybridization

Femura and tibias dissected from animals were fixed in 10% neutral buffered formalin for 2 days, decalcified in 10% EDTA (PTH 7.4) for 3 weeks, and then embedded in paraffin. Longitudinally oriented, 4-μm-thick sections including growth plate and metaphysis were deparaffinized and rehydrated, and then processed for H&E (Thermo Fisher Scientific, Pittsburgh, PA, USA) staining, Goldner's trichrome staining, TRAP (Sigma-Aldrich, St. Louis, MO, USA) staining, safranin O (Sigma-Aldrich) staining, or immunostaining using primary antibodies against PECAM-1 (Abcam, Cambridge, MA, USA) and VEGFR2 (Cell Signaling, Danvers, MA, USA). A horseradish-peroxidase-streptavidin detection system (Dako, Glostrup, Denmark) was used to detect immunoactivity, followed by counterstaining with hematoxylin (Dako) or methyl green (Sigma-Aldrich). For evaluation of proliferation, 50μg of BrdU per gram of body weight was given to mice ip 2 hours before death. BrdU was detected using BrdU staining kit (Invitrogen, Carlsbad, CA, USA). The BrdU labeling index was calculated as the ratio of BrdU-positive nuclei over total nuclei of chondrocytes in the growth plate. For evaluation of apoptosis, apoptotic chondrocytes were identified using by a TUNEL-based in situ cell death detection kit (Roche, Mannheim, Germany).

Percentage of TUNEL-positive chondrocytes over total number of chondrocytes in the growth plate was calculated. For evaluation of gene expression, nonradioactive in situ hybridization was performed according to the DIG application manual of the manufacturer (Roche). The digoxigenin-labeled RNA probes for Col X, MMP13, Ihh, and PTH1R were synthesized using a DIG RNA labeling kit (sp6/T7) (Roche) and detected using a DIG nucleic acid detection kit (Roche).

Micro–computed tomography (μCT) and histomorphometric analysis

Femura and tibias obtained from mice were dissected free of soft tissue, fixed overnight in 70% ethanol, and analyzed by a highresolution μCT (SkyScan 1076 in vivo CT, SkyScan, Aartselaar, Belgium) installed with software NRecon v1.6, CTan v1.9, and CTVol v2.0. The scanner was set at a voltage of 89 kVp, a current of 112 uA, and a resolution of 8.67 μm per pixel. Cross-sectional images of the proximal tibias were used to perform 3D histomorphometric analysis of trabecular and cortical bone. The sample area of trabecular bone selected for scanning was a 1.5-mm length of metaphyseal primary spongiosa,

Author Manuscript Author Manuscript Author Manuscript Author Manuscript

originating 0.5 mm below the lowest point of growth plate and extending caudally. The area of interest for cortex was 1.0 to 5.0 mm from the growth plate. The 2D parameters including the number of osteoblasts and osteoclasts and labeling indexes of PECAM-1 or VEGFR2 were determined by quantitative histomorphometric GA. The numbers of osteoblasts and osteoclasts were analyzed at the trabecular bone. The PECAM-1- or VEGFR2-positive cells were counted in 300 μm from the growth plates and calculated as the ratio of over total numbers of chondrocyte columns. In addition, the invasion occurrence was the ratio of PECAM-1-positive chondrocyte lacunae over total chondrocyte lacunae. Four randomly selected visual fields per specimen, in three specimens per mouse in each group, were measured.

Imaging of blood vessels in bone

Blood vessels in bone were imaged by angiography of Microphil-perfused long bones.[24] The vasculature was flushed with 0.9% normal saline containing heparin sodium (100 U/mL) at a pressure of 100 mmHg through a needle inserted into the ventricle. The specimens were then stored at 4°C overnight for contrast agent polymerization. Mouse tibias were dissected from the specimens and soaked in 10% neutral buffered formalin for 2 days to ensure the tissue fixation. Specimens were subsequently treated in 10% EDTA (PTH 7.4) to decalcify the bone and facilitate image thresholding of tibia vasculature from the bone. Images were obtained using the μCT. The 3D histomorphometric parameters, including vessel volume, vessel number, and vessel concentration, were evaluated.

Double calcein labeling

Double calcein labeling was performed by intraperitoneal injection of mice with two sequential doses of calcein (Sigma-Aldrich; 10 mg kg^{-1} in 2% sodium bicarbonate in sterile saline) 3 and 9 days before euthanization. Bones were harvested and embedded in Tissue-Tek (Sakura, Torrance, CA, USA) acrylic resin. Serial sections were cut, and the freshly cut surface of each section was imaged using fluorescence microscopy. BFR/BV at cortex and trabeculae was measured using OsteoMeasureXP. Four randomly selected visual fields per specimen, in three specimens per mouse in each group, were measured.

Gene expression analysis

Primary osteoblasts were isolated from calvariae of newborn mice as previously described.[24] Total RNA was prepared with Trizols reagent (Sigma), followed by DNase treatment and reverse-transcription into cDNA using random hexaprimers. Quantitative RT-PCR on 5 ng of amplified cDNA was performed on a Bio-Rad (Hercules, CA, USA) real-time thermal cycler CFX96 using SYBR GREEN PCR Master Mix (Promega, San Luis Obispo, CA, USA). The primers for *VEGFa* and *angiopoietin-1* were previously described.[25] Relative gene expression was calculated using the ΔΔCT method normalized to GAPDH levels for each individual sample measured in triplicate.

Statistical analysis

Statistical differences between two groups of data were analyzed with Student's *t* test. Data are presented as means ± SD.

Author Manuscript Author Manuscript Author Manuscript Author Manuscript

Results

Growth retardation of postnatal long bone in osteoblastic PTH1R knockout mice

To evaluate the potential role of osteoblastic PTH1R signaling on longitudinal growth of long bone, the PTH1R gene was selectively deleted in osteoblasts by crossing floxed PTH1R mice with Cre-transgenic mice driven by an osteocalcin promoter (*OC-Cre*).[21] Although mice lacking PTH1R ($PTH1R^{-/-}$) were indistinguishable in size and body weight from their wild-type littermates ($PTH1R^{+/+}$) at birth, by 4 weeks of age, $PTH1R^{-/-}$ mice were noted to have a lower body weight (Fig. 1*A*) and shorter femoral length (Fig. 1*B, C*). The $PTH1R^{-/-}$ femora exhibited abnormal widening of both the proximal and distal metaphysis. The short stature and low bone mass remained apparent in 8-month-old mice (Fig. 1*D*). Kyphosis was also observed (Fig. 1*D*, white arrowheads), indicating a softening of bone and impaired bone metabolism. These results showed that the growth of long bone was impaired in $PTH1R^{-/-}$ mice.

Disrupted bone formation in $PTH1R^{-/-}$ mice

Analysis of the metaphyseal region of long bones revealed that the trabecular volume was significantly decreased in 4-week-old $PTH1R^{-/-}$ mice relative to their wild-type littermates (Fig. 2*A*, left two panels; *B*), whereas the cortical bone exhibited progressive thickening from diaphysis toward metaphysis (Fig. 2*A*, right two panels; *C*).

Dynamic analysis of bone formation with double calcein labeling revealed that bone mineralization at trabeculae and periosteal surfaces were reduced, whereas $PTH1R^{-/-}$ endosteum exhibited accelerated bone formation (Fig. 2*D–F*). Quantification of osteoblast and osteoclast numbers at trabeculae showed that they were both decreased (Fig. 2*G, H*), with osteoblasts showing a reduction in number at a younger age compared with osteoclasts (4 versus 8 weeks) (Fig. 2*G, H*). These data demonstrate that the disruption of PTH1R reduces osteoblast activity and restrains trabecular bone formation.

Defects in hypertrophic differentiation of chondrocytes in $PTH1R^{-/-}$ mice

To understand the impaired growth of long bone, we analyzed the growth plate chondrocytes in the proximal tibia of mice at different ages using H&E and safranin O staining. At 1 week of age, the proliferating and hypertrophic zones were indistinguishable between $PTH1R^{-/-}$ mice and their wild-type littermates (Fig. 3*A*). However, a distinct phenotype was observed by 4 weeks of age, where an apparent loss of hypertrophic morphology and disruption of the columnar organization of chondrocytes emerged in $PTH1R^{-/-}$ growth plates (Fig. 3*B*, arrows). The defect in chondrocytes progressed with age such that by 8 weeks, the columnar arrangement of growth plate chondrocytes was completely disrupted, and the remaining cartilage was discontinuous and disorganized, with bridging of bone between the epiphyseal bone and the primary spongiosa, indicating fusion of the growth plate in the $PTH1R^{-/-}$ mice (Fig. 3*C*). These data demonstrate an aberrant phenotype of growth plate cartilage when PTH1R signaling is deleted in osteoblasts.

Author Manuscript Author Manuscript Author Manuscript Author Manuscript

Abnormalities of gene expression in *PTH1R*$^{-/-}$ growth cartilage

We measured the expression patterns of multiple chondrocyte differentiation markers using in situ hybridization analysis. Expression of collagen X (ColX), a marker of hypertrophic chondrocytes, was largely decreased in 4-week-old *PTH1R*$^{-/-}$ mice relative to controls (Fig. 4*A*). Matrix metalloproteinase-13 (MMP13) was also decreased (Fig. 4*B*).

Additionally, expression of indian hedgehog (Ihh) was downregulated but more diffusely distributed relative to wild-type controls, suggestive of an expanded prehypertrophic zone, likely owing to acceleration in early differentiation or lack of further hypertrophy (Fig. 4*C*). Furthermore, PTH1R expression in cartilage was slightly downregulated (Fig. 4*D*, Supplemental Fig. S1), even though its expression in primary spongiosa was eliminated by OC-Cre-driven deletion (Fig. 4*D*, Supplemental Fig. S2). To test if the decreased number of hypertrophic chondrocytes was attributable to decreased chondrocyte proliferation, increased apoptosis, or both, BrdU labeling and TUNEL staining were performed. In *PTH1R*$^{-/-}$ mice, BrdU-positive cells were less concentrated in proliferative columns but more diffusely distributed, although the total number of proliferating chondrocytes was not changed significantly (Fig. 4*E, F*). TUNEL staining of the chondrocytes at the chondro-osseous junction revealed an increase in number of hypertrophic chondrocytes undergoing apoptosis in *PTH1R*$^{-/-}$ mice compared with wild-type controls (Fig. 4*G, H*). Thus, these results indicate that deletion of PTH1R in osteoblasts impaired chondrocyte function, leading to decreased number of hypertrophic chondrocytes in the growth plate.

Impaired angiogenesis and vascular invasion in *PTH1R*$^{-/-}$ mice

Angiogenesis and vascular invasion of growth plate are essential processes for development and remodeling of cartilage. To evaluate whether PTH receptor signaling in osteoblasts regulates angiogenesis during endochondral bone growth, we performed μCT angiography on mice at 4 weeks of age using Microfil. Vascularity was dramatically decreased in *PTH1R*$^{-/-}$ mice (Fig. 5*A*, upper panels), as evidenced by quantitative analysis showing that vessel volume, number, and connectivity were significantly reduced (Fig. 5*B–D*). The *PTH1R*$^{-/-}$ blood vessels were disorganized and exhibited a dysplastic pattern beneath the center of the growth plate. Concomitantly, a penetration of bone into cartilage occurred in *PTH1R*$^{-/-}$ mice, resulting in early fusion of bones between the primary and secondary ossification centers (Fig. 5*A*, arrows in right panels). To assess the vascular invasion of growth plate, we performed histological staining for PECAM-1, which is expressed specifically by vascular endothelial cells. We found that 52% ± 5.9% of capillaries expressing PECAM-1 did not extend into the hypertrophic chondrocytes in *PTH1R*$^{-/-}$ mice (Fig. 5*E*, upper panels; *F*), and red blood cells were markedly reduced in *PTH1R*$^{-/-}$ lacunae left from apoptosis of hypertrophic chondrocytes (Fig. 5*E*, lower panels). Thus, the deletion of PTH1R in osteoblasts resulted in impaired endochondral vasculature formation and invasion. To evaluate angiogenic activity of PTH1R in osteoblasts, we analyzed expression levels of VEGFa and angiopoietin-1, two pro-angiogenic factors, in primary osteoblasts. Both of them were significantly decreased in *PTH1R*$^{-/-}$ osteoblasts compared with *PTH1R*$^{+/+}$ controls (Fig. 5*G, H*), implying a role of osteoblastic PTH1R signaling in stimulation of angiogenic response. Together, these results demonstrate that PTH1R in

Author Manuscript Author Manuscript Author Manuscript Author Manuscript

osteoblasts is necessary for maintenance of endochondral angiogenesis and vascular invasion of cartilage.

Disruption of vascularization alone leads to a decrease in number of hypertrophic chondrocytes

To determine the sequence of events leading to the observed phenotypes, we studied additional mouse models that have targeted disruption of the vasculature or increased PTH signaling in bone. PECAM-1 deficiency is reported to specifically and moderately affect vascularization.[26,27] We confirmed that the number of vascular endothelial cells was decreased in 8-week-old *PECAM-1*$^{-/-}$ mice compared with wild-type littermates (*PECAM-1*$^{+/+}$) by immunostaining for the vascular marker VEGFR2 (Fig. 6*A*, lower panels; *B*). The *PECAM-1*$^{-/-}$ mice exhibited a similar, yet less severe, bone phenotype to that found in *PTH1R*$^{-/-}$ mice, including reduced trabecular bone formation (Fig. 6*A*, upper panels; *C, D*) and bony invasion into the cartilage (Fig. 6*A*, arrow; *E*). H&E and safranin O staining of proximal tibia from *PECAM-1*$^{-/-}$ mice showed a decrease in the number of hypertrophic chondrocytes, which was further confirmed by attenuated expression of ColX (Fig. 6*F, G*). Accordingly, the number of hypertrophic chondrocytes undergoing apoptosis was increased (Fig. 6*H*). These data suggest that the disruption of vasculature alone restrains hypertrophic development of chondrocytes. To further address the role of the vascularization in mediating PTH effect on cartilage, we analyzed the mice lacking TGFβ type II receptor (TβRII) in mature osteoblasts, in which PTH signaling has been shown to be hyperactive in osteoblasts.[9] TβRII$^{-/-}$ mice exhibited increased blood vessels as evidenced by increased PECAM-1 staining (Fig. 6*I*, upper panels; *J*). Concurrently, the hypertrophy of chondrocytes was augmented (Fig. 6*I*, lower panels; *K*), supporting that the endochondral vascularization is coupled with the maturation of chondrocytes. Therefore, PTH receptor signaling in osteoblasts likely supports chondrocyte hypertrophy through PTH-mediated endochondral vascular angiogenesis and invasion.

Discussion

Endochondral ossification is a fundamental process that occurs during development of long bones and contributes to longitudinal growth. This process involves a carefully regulated sequence of changes in chondrocyte behavior[28] and co-invasion of cartilage by blood vessels and osteoblast precursors.[29] The osteoblast-mediated bone formation subsequently establishes the primary ossification center. We found that disruption of PTH1R signaling in osteoblasts decreased the numbers of osteoblasts and osteoclasts and disrupted the trabecular bone formation. Importantly, endochondral angiogenesis and vascular invasion of the cartilage were impaired, and hypertrophic development of chondrocytes was attenuated. These changes cumulatively led to premature fusion of the growth plate, with resultant short limbs. Thus, PTH1R signaling in osteoblastic cells regulates endochondral vascularization in maintenance of postnatal growth plate (Fig. 6*L*).

We observed a positive correlation between angiogenesis and chondrocyte hypertrophy in *PTH1R*$^{-/-}$, *PECAM-1*$^{-/-}$, and *TβRII*$^{-/-}$ mice, even though the altered vascularization was not the only manifestation in these animals. Consistently, endothelial-cell-specific disruption

Author Manuscript Author Manuscript Author Manuscript Author Manuscript

of Notch signaling impaired bone vessel growth and led to defects of chondrocytes and shortening of long bones.[30] In osteoarthritis, increased vascular invasion is associated with accelerated maturation and hypertrophy of chondrocytes.[31,32] Additionally, chick embryos treated with squalamine, an inhibitor of angiogenesis, exhibited delayed chondrocyte differentiation.[33] Therefore, PTH1R signaling in osteoblasts, by enhancing vascularization, may positively regulate chondrocyte maturation.

During embryonic development, however, inhibition of vascularization by systemic administration of VEGF inhibitor[34] or chondrocyte-specific deletion of VEGF resulted in delayed removal of terminal chondrocytes and expanded hypertrophic zone.[35] Notably, global knockout of PTH also led to expansion of the hypertrophic zone in newborn pups.[3] This phenotype was not found in *PTH1R*$^{-/-}$ mice at 4 to 8 weeks of age, suggesting that additional postnatal factors are involved in regulation of chondrocytes in *PTH1R*$^{-/-}$ mice. Possible factors include changes in counter-regulatory mechanisms between mouse models employed, differential temporal and spatial signaling effects, or direct interactions between osteoblasts and chondrocytes. We found increased apoptosis at chondro-osseous junction in *PTH1R*$^{-/-}$ mice, suggesting PTH1R signaling in osteoblasts may have a direct role in mediating chondrocyte survival. Further studies are needed to explore each of these potential mechanisms further.

PTH and parathyroid hormone–related peptide (PTHrP) both bind to the PTH1R. PTH is an endocrine hormone, whereas PTHrP acts in an autocrine and/or paracrine manner. Both have been shown to stimulate PTH1R in osteoblasts.[36,37] Because PTHrP is detected before development of the parathyroid glands (E11.5–E12.5 versus E14.5–15.5),[2] it is more involved in embryonic growth rather than PTH, specifically regulating fetal-placental calcium homeostasis[38] and delaying chondrocyte differentiation.[28]

Occurrence of the parathyroid glands reflects a requirement of additional systemic control on calcium homeostasis and limb development in postnatal life and may play a role in synchronizing the growth rates of corresponding bones in the body. Modulation of chondrocyte hypertrophy by PTH1R signaling in osteoblasts could be a complementary mechanism for either PTH or PTHrP in maintaining the cartilage for elongation of bone. Indeed, both ligands have been shown to regulate longitudinal growth in mice. Deletion of PTH and PTHrP independently impair long bone growth with an even more dramatic decrease in the length of long bones when both were deleted simultaneously.[3]

We used the OC-Cre to target PTH1R deletion in osteoblasts. The expression of OC-Cre was analyzed in YFP florescence using OC-Cre/Rosa26-YFP mice (Supplemental Fig. S2). In addition to expression of OC-Cre in osteoblasts and osteocytes, some weak clustered OC-Cre signals were also noticed in proliferating chondrocytes, in line with the previous observation,[20] implying that a mosaic expression of OC-Cre may interfere with the *PTH1R*$^{-/-}$ phenotype. PTH1R signaling in proliferating chondrocytes has been shown to stimulate proliferation of chondrocytes and delay maturation.[4,17–19] Therefore, inactivation of PTH1R in chondrocytes would be expected to accelerate differentiation of chondrocytes with expansion of the hypertrophic zone. The contrary hypertrophic phenotype we observed in the *PTH1R*$^{-/-}$ mice was, therefore, unlikely the result of nonspecific deletion of

Author Manuscript Author Manuscript Author Manuscript Author Manuscript

chondrocyte *PTH1R*. In addition, the mosaic expression of OC-Cre did not interfere significantly in the chondrocyte morphology of 1-week-old *PTH1R*$^{-/-}$ growth plate, suggesting that the cartilage was not adversely affected during the embryonic stage of development. Specifically, the aberrant phenotype of cartilage emerged only in postnatal life, along with turnover of trabecular bone in *PTH1R*$^{-/-}$ mice.

Trabecular bone is a transient structure during bone development. The generation of trabecular bone tightly couples with that of the growth plate cartilage, and both continue until growth ceases in early adulthood. Thus, trabecular bone and cartilage may form integrated working machinery, producing the growth of bone. Our study implies that osteoblastic PTH1R signaling may play an evolutionary role in modifications of the skeleton to allow for the growth of limbs and provides insight for future studies to further dissect the cell signaling mechanisms that couple chondrogenesis, angiogenesis, and osteogenesis during longitudinal bone growth.

Supplementary Material

Refer to Web version on PubMed Central for supplementary material.

Acknowledgments

We gratefully acknowledge Henry Kronenberg for *PTH1R*$^{flox/flox}$ mice; Thomas Clemens for OC-Cre mice; Harold Moses for *TβRII*$^{flox/flox}$ mice; and Gehua Zhen and Michael Luo for technical assistance. This work was supported by National Institutes of Health grant AR060433 (to TQ), AR063943(XC) and DK057501 (XC).

Authors' roles: T. Q. performed most of the experiments, analysed data and prepared the manuscript. L. X., J. C., and C. W. performed some of the experiments. M. H., P. N., and W. L. provided some experimental materials. J. C. and X. C. prepared the manuscript.

References

1. Bergwitz C, Klein P, Kohno H, et al. Identification, functional characterization, and developmental expression of two nonallelic parathyroid hormone (PTH)/PTH-related peptide receptor isoforms in *Xenopus laevis* (Daudin). Endocrinology. 1998; 139(2):723–32. [PubMed: 9449646]
2. Kaufman, MH. The atlas of mouse development. Academic Press; San Diego: 1992.
3. Miao D, He B, Karaplis AC, Goltzman D. Parathyroid hormone is essential for normal fetal bone formation. J Clin Invest. 2002; 109(9):1173–82. [PubMed: 11994406]
4. Hirai T, Chagin AS, Kobayashi T, Mackem S, Kronenberg HM. Parathyroid hormone/parathyroid hormone-related protein receptor signaling is required for maintenance of the growth plate in postnatal life. Proc Natl Acad Sci USA. 2011; 108(1):191–6. [PubMed: 21173257]
5. Jobert AS, Zhang P, Couvineau A, et al. Absence of functional receptors for parathyroid hormone and parathyroid hormone-related peptide in Blomstrand chondrodysplasia. J Clin Invest. 1998; 102(1):34–40. [PubMed: 9649554]
6. Schipani E, Langman CB, Parfitt AM, et al. Constitutively activated receptors for parathyroid hormone and parathyroid hormone-related peptide in Jansen's metaphyseal chondrodysplasia. N Engl J Med. 1996; 335(10):708–14. [PubMed: 8703170]
7. Namnoum AB, Merriam GR, Moses AM, Levine MA. Reproductive dysfunction in women with Albright's hereditary osteodystrophy. J Clin Endocrinol Metab. 1998; 83(3):824–9. [PubMed: 9506735]
8. Patten JL, Johns DR, Valle D, et al. Mutation in the gene encoding the stimulatory G protein of adenylate cyclase in Albright's hereditary osteodystrophy. N Engl J Med. 1990; 322(20):1412–9. [PubMed: 2109828]

Author Manuscript Author Manuscript Author Manuscript Author Manuscript

9. Qiu T, Wu X, Zhang F, Clemens TL, Wan M, Cao X. TGF-beta type II receptor phosphorylates PTH receptor to integrate bone remodelling signalling. Nat Cell Biol. 2010; 12(3):224–34. [PubMed: 20139972]
10. Wan M, Yang C, Li J, et al. Parathyroid hormone signaling through low-density lipoprotein-related protein 6. Genes Dev. 2008; 22(21):2968–79. [PubMed: 18981475]
11. Yu B, Zhao X, Yang C, et al. Parathyroid hormone induces differentiation of mesenchymal stromal/stem cells by enhancing bone morphogenetic protein signaling. J Bone Miner Res. 2012; 27(9):2001–14. [PubMed: 22589223]
12. Bikle DD, Sakata T, Leary C, et al. Insulin-like growth factor I is required for the anabolic actions of parathyroid hormone on mouse bone. J Bone Miner Res. 2002; 17(9):1570–8. [PubMed: 12211426]
13. Canalis E, Centrella M, Burch W, McCarthy TL. Insulin-like growth factor I mediates selective anabolic effects of parathyroid hormone in bone cultures. J Clin Invest. 1989; 83(1):60–5. [PubMed: 2910920]
14. Prisby R, Guignandon A, Vanden-Bossche A, et al. Intermittent PTH(1–84) is osteoanabolic but not osteoangiogenic and relocates bone marrow blood vessels closer to bone-forming sites. J Bone Miner Res. 2011; 26(11):2583–96. [PubMed: 21713994]
15. Calvi LM, Adams GB, Weibrecht KW, et al. Osteoblastic cells regulate the haematopoietic stem cell niche. Nature. 2003; 425(6960):841–6. [PubMed: 14574413]
16. Mendez-Ferrer S, Michurina TV, Ferraro F, et al. Mesenchymal and haematopoietic stem cells form a unique bone marrow niche. Nature. 2010; 466(7308):829–34. [PubMed: 20703299]
17. Lanske B, Karaplis AC, Lee K, et al. PTH/PTHrP receptor in early development and Indian hedgehog-regulated bone growth. Science. 1996; 273(5275):663–6. [PubMed: 8662561]
18. Guo J, Chung UI, Yang D, Karsenty G, Bringhurst FR, Kronenberg HM. PTH/PTHrP receptor delays chondrocyte hypertrophy via both Runx2-dependent and -independent pathways. Dev Biol. 2006; 292(1):116–28. [PubMed: 16476422]
19. Guo J, Chung UI, Kondo H, Bringhurst FR, Kronenberg HM. The PTH/PTHrP receptor can delay chondrocyte hypertrophy in vivo without activating phospholipase C. Dev Cell. 2002; 3(2):183–94. [PubMed: 12194850]
20. Kobayashi T, Chung UI, Schipani E, et al. PTHrP and Indian hedgehog control differentiation of growth plate chondrocytes at multiple steps. Development. 2002; 129(12):2977–86. [PubMed: 12050144]
21. Zhang M, Xuan S, Bouxsein ML, et al. Osteoblast-specific knockout of the insulin-like growth factor (IGF) receptor gene reveals an essential role of IGF signaling in bone matrix mineralization. J Biol Chem. 2002; 277(46):44005–12. [PubMed: 12215457]
22. Duncan GS, Andrew DP, Takimoto H, et al. Genetic evidence for functional redundancy of Platelet/Endothelial cell adhesion molecule-1 (PECAM-1): CD31-deficient mice reveal PECAM-1-dependent and PECAM-1-independent functions. J Immunol. 1999; 162(5):3022–30. [PubMed: 10072554]
23. Newman PJ. The role of PECAM-1 in vascular cell biology. Ann NY Acad Sci. 1994; 714:165–74. [PubMed: 8017765]
24. Zhang F, Qiu T, Wu X, et al. Sustained BMP signaling in osteoblasts stimulates bone formation by promoting angiogenesis and osteoblast differentiation. J Bone Miner Res. 2009; 24(7):1224–33. [PubMed: 19257813]
25. Jeansson M, Gawlik A, Anderson G, et al. Angiopoietin-1 is essential in mouse vasculature during development and in response to injury. J Clin Invest. 2011; 121(6):2278–89. [PubMed: 21606590]
26. Cao G, Fehrenbach ML, Williams JT, Finklestein JM, Zhu JX, Delisser HM. Angiogenesis in platelet endothelial cell adhesion molecule-1-null mice. Am J Pathol. 2009; 175(2):903–15. [PubMed: 19574426]
27. Dimaio TA, Wang S, Huang Q, Scheef EA, Sorenson CM, Sheibani N. Attenuation of retinal vascular development and neovascularization in PECAM-1- deficient mice. Dev Biol. 2008; 315(1):72–88. [PubMed: 18206868]
28. Kronenberg HM. Developmental regulation of the growth plate. Nature. 2003; 423(6937):332–6. [PubMed: 12748651]

Author Manuscript Author Manuscript Author Manuscript Author Manuscript

29. Maes C, Kobayashi T, Selig MK, et al. Osteoblast precursors, but not mature osteoblasts, move into developing and fractured bones along with invading blood vessels. Dev Cell. 2010; 19(2): 329–44. [PubMed: 20708594]

30. Ramasamy SK, Kusumbe AP, Wang L, Adams RH. Endothelial Notch activity promotes angiogenesis and osteogenesis in bone. Nature. 2014; 507(7492):376–80. [PubMed: 24647000]

31. Pesesse L, Sanchez C, Henrotin Y. Osteochondral plate angiogenesis: a new treatment target in osteoarthritis. Joint Bone Spine. 2011; 78(2):144–9. [PubMed: 20851653]

32. Lories RJ, Luyten FP. The bone-cartilage unit in osteoarthritis. Nat Rev Rheumatol. 2011; 7(1):43–9. [PubMed: 21135881]

33. Yin M, Gentili C, Koyama E, Zasloff M, Pacifici M. Antiangiogenic treatment delays chondrocyte maturation and bone formation during limb skeletogenesis. J Bone Miner Res. 2002; 17(1):56–65. [PubMed: 11771670]

34. Gerber HP, Vu TH, Ryan AM, Kowalski J, Werb Z, Ferrara N. VEGF couples hypertrophic cartilage remodeling, ossification and angiogenesis during endochondral bone formation. Nat Med. 1999; 5(6):623–8. [PubMed: 10371499]

35. Zelzer E, Mamluk R, Ferrara N, Johnson RS, Schipani E, Olsen BR. VEGFA is necessary for chondrocyte survival during bone development. Development. 2004; 131(9):2161–71. [PubMed: 15073147]

36. Martin TJ. Osteoblast-derived PTHrP is a physiological regulator of bone formation. J Clin Invest. 2005; 115(9):2322–4. [PubMed: 16138187]

37. Miao D, Li J, Xue Y, Su H, Karaplis AC, Goltzman D. Parathyroid hormone-related peptide is required for increased trabecular bone volume in parathyroid hormone-null mice. Endocrinology. 2004; 145(8):3554–62. [PubMed: 15090463]

38. Kovacs CS, Manley NR, Moseley JM, Martin TJ, Kronenberg HM. Fetal parathyroids are not required to maintain placental calcium transport. J Clin Invest. 2001; 107(8):1007–15. [PubMed: 11306604]

Author Manuscript Author Manuscript Author Manuscript Author Manuscript

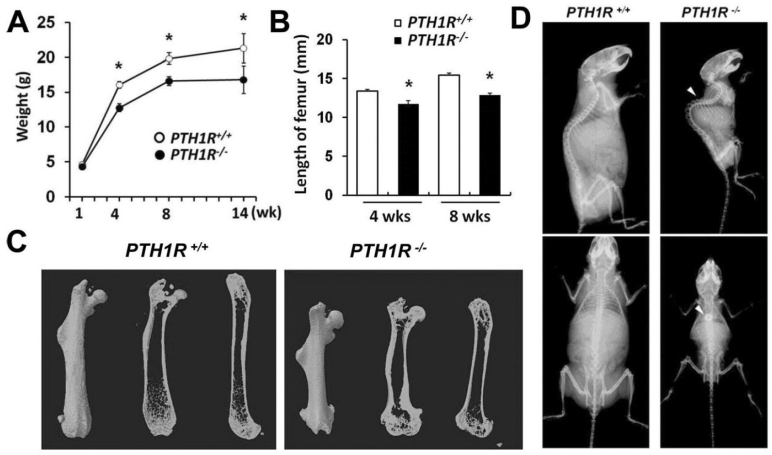

Fig. 1.

PTH1R$^{-/-}$ mice developed postnatal growth retardation of long bone. (*A*, *B*) Analysis of body weight and femur length of *PTH1R*$^{+/+}$ and *PTH1R*$^{-/-}$ mice at different weeks of age. (*C*) Three-dimensional reconstruction of the femura from μCT scans of 8-week-old mice. (*D*) Faxitron radiographs of whole bodies from 8-month-old mice showing kyphosis (as indicated by white arrowheads).

Author Manuscript Author Manuscript Author Manuscript Author Manuscript

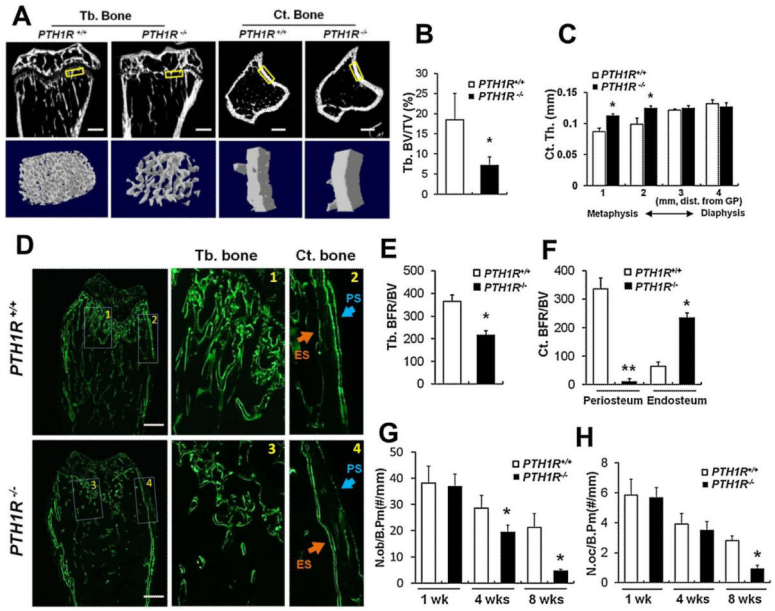

Fig. 2.

Impaired bone formation in *PTH1R*$^{-/-}$ mice. (*A*) Longitudinal sections and cross sections at proximal tibias from μCT scans on 4-week-old *PTH1R*$^{+/+}$ and *PTH1R*$^{-/-}$ mice (upper) and three-dimensional reconstruction of selected areas (boxed) representing trabecular bone and cortical bone (lower). Scale bars=300 μm. (*B*, *C*) Quantitative μCT analysis on trabecular bone volume (*B*) and cortical bone thickness (*C*) at proximal tibias. (*D*) Calcein double labeling showing distinct bone formation at trabecular bone and cortical bone in proximal femura from 4-week-old mice. 1–4: magnified views of the boxed areas at metaphyseal trabecular bone (1 and 3) and cortical bone (2 and 4). ES=endosteal surface; PS=periosteal surface. Scale bars=500 μm. (*E*, *F*) Quantification of bone formation rates at trabecular bone (*E*) and cortical bone (*F*). (*G*, *H*) Measurement of the numbers of osteoblasts (*G*) and osteoclasts (*H*) at the proximal tibias in mice at 1, 4, and 8 weeks of age. Data shown represent means±SD for five animals per group. **p*<0.05 versus *PTH1R*$^{+/+}$; ***p*<0.01 versus *PTH1R*$^{+/+}$.

Author Manuscript Author Manuscript Author Manuscript Author Manuscript

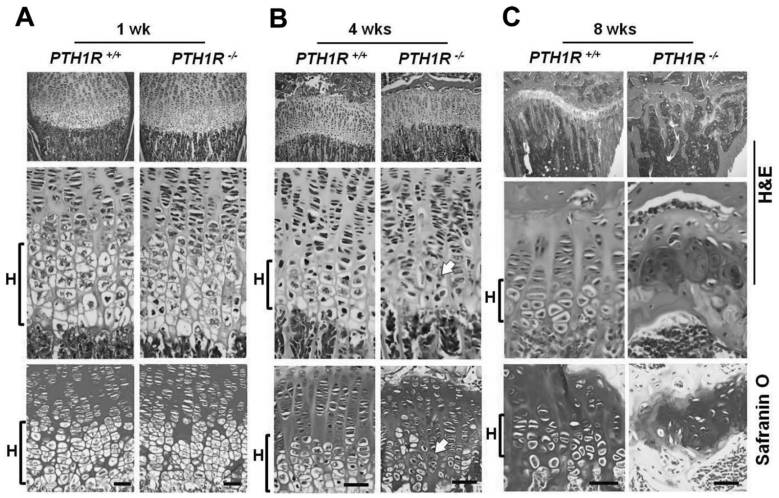

Fig. 3.

Profound defect in hypertrophic differentiation of chondrocytes in *PTH1R*$^{-/-}$ mice. (*A–C*) H&E (upper two panels) and safranin O (bottom panels) staining of proximal growth plates of the tibia from *PTH1R*$^{+/+}$ and *PTH1R*$^{-/-}$ mice at 1, 4 and 8 weeks of age. H=hypertrophic zone. Scale bars=50 μm.

Author Manuscript Author Manuscript Author Manuscript Author Manuscript

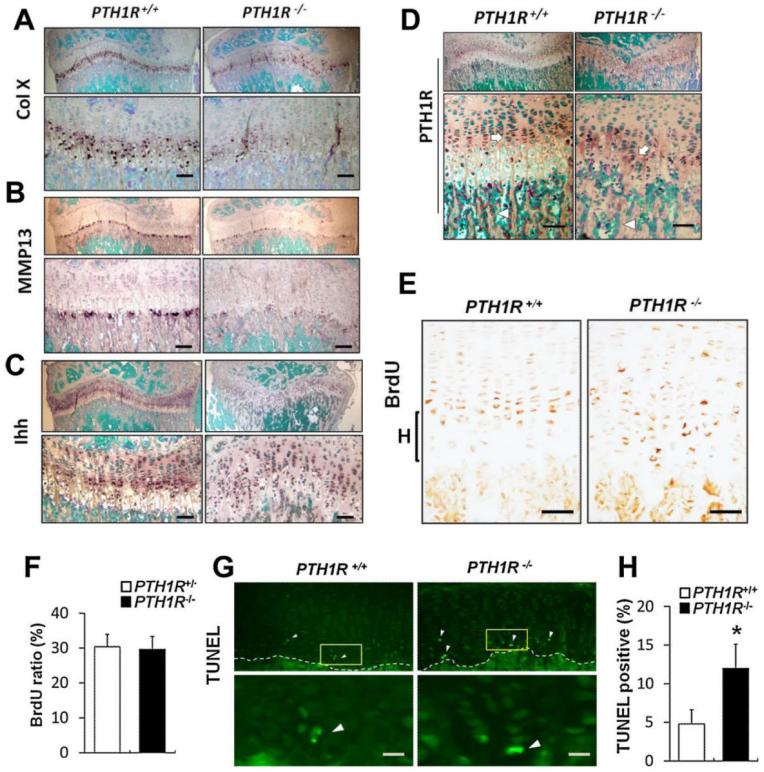

Fig. 4.

Abnormalities of gene expression in growth cartilage from 4-week-old *PTH1R*$^{-/-}$ mice. (*A–D*) Expression patterns of ColX (*A*), MMP13 (*B*), Ihh (*C*), and PTH1R (*D*) in sections of the growth plates, as analyzed by nonradioactive in situ hybridization. Sections were counterstained with methyl green. The mRNA signal is shown as a dark brown precipitate. Lower panels are magnified view of upper panels. Scale bars=50 μm. Arrow=proliferating chondrocytes. Arrowheads=bone-surface osteoblasts. (*E*) BrdU labeling at the proximal growth plate of tibias showed that BrdU-positive chondrocytes (brown) were less concentrated but more diffusely distributed. Scale bars=50 μm. (*F*) Quantification of the percentage of BrdU-positive nuclei. (*G*) TUNEL staining at chondro-osseous junction revealed an increase in number of TUNEL-positive (green) chondrocytes, as indicated by white arrowheads. (*H*) Quantification of the percentage of TUNEL-positive cells. Scale bars=20 μm. Data shown represent means±SD for six animals per group. *p<0.05 versus *PTH1R*$^{+/+}$.

Author Manuscript Author Manuscript Author Manuscript Author Manuscript

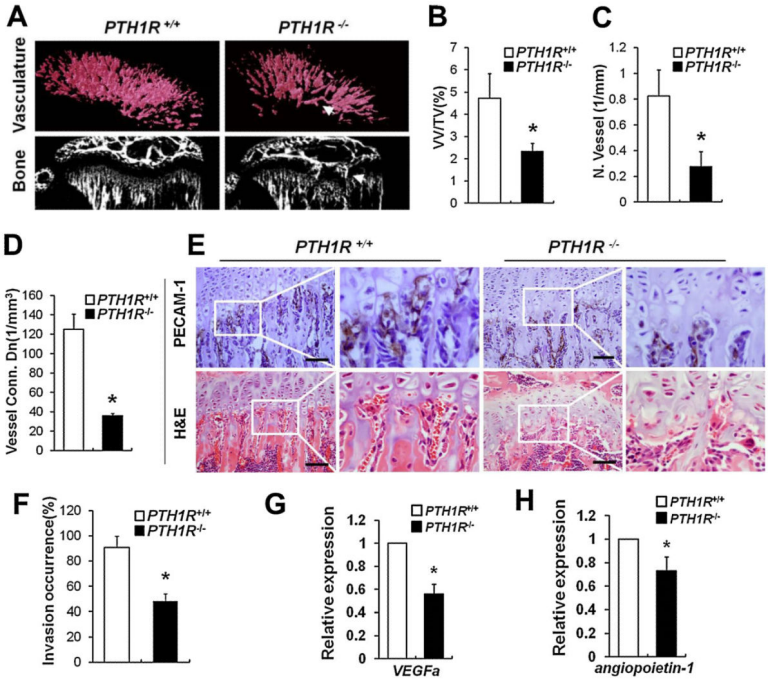

Fig. 5.

Impaired angiogenesis and vascular invasion in 4-week-old *PTH1R*$^{-/-}$ mice. (*A*) Impaired angiogenesis in femoral metaphysis. Upper panels, μCT images of Microfil-perfused vasculature underneath the growth plates showed impaired vascularity and a dysplastic pattern beneath the center of growth plate (arrow); lower panels, μCT images of bone showed that a penetration of bone into cartilage occurred (arrow). (*B–D*) Quantifications of vessel volume per total volume (*B*), vessel number (*C*), and vessel concentration (*D*). (*E*) PECAM-1 and H&E staining of the chondro-osseous junctions. Magnified views of the boxed areas are shown on the right. (*F*) Quantitative evaluations of vascular invasion. (*G, H*) Relative mRNA levels of VEGFa (*G*) and angiopoietin-1 (*H*) in primary osteoblasts. Scale bars=50 μm. Data shown represent means±SD for five animals per group. *p<0.05 versus *PTH1R*$^{+/+}$.

Author Manuscript Author Manuscript Author Manuscript Author Manuscript

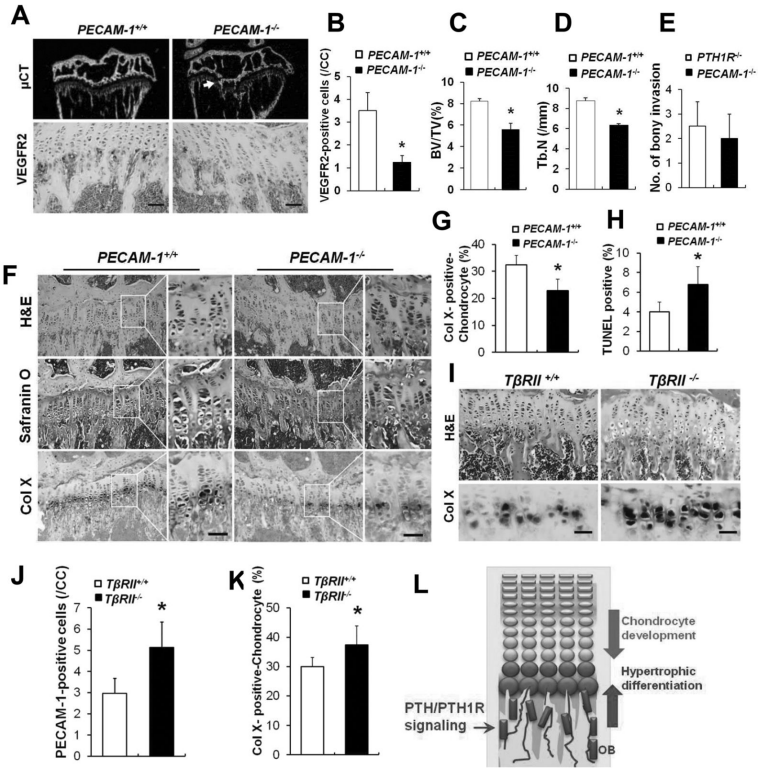

Fig. 6.

Disruption of vascularization alone restrains hypertrophic differentiation of chondrocytes. (*A*) μCT images and VEGFR2-stained sections of the proximal tibias from 8-week-old *PECAM-1*$^{+/+}$ and *PECAM-1*$^{-/-}$ mice. A penetration of bone into cartilage of *PTH1R*$^{-/-}$ mice is shown (arrow). (*B*) Quantification of VEGFR2-positive cells per chondrocyte column (CC). (*C, D*) Trabecular bone volume (*C*) and number (*D*) at the tibial metaphysis. (*E*) Number of bony invasion of cartilage. (*F*) H&E and safranin O staining of growth cartilage and in situ hybridization for Col X. (*G*) Quantification of the percentage of Col X-positive chondrocytes in the proximal growth plate of the tibias. (*H*) Quantification of the percentage of TUNEL-positive cells. (*I*) H&E staining and in situ hybridization for Col X at the chondro-osseous junctions from 8-week-old *TβRII*$^{+/+}$ and *TβRII*$^{-/-}$ mice. (*J*) Quantification of PECAM-1–positive cells per chondrocyte column (CC). (*K*) Quantification of the percentage of Col X-positive chondrocytes in the proximal growth plate of the tibias. (*L*) Model for role of PTH/PTH1R signaling in maintaining growth plate cartilage in postnatal growth of bone. OB=osteoblasts. Scale bars=50 μm. Data shown represent means±SD for three animals per group. *p<0.05 versus *PTH1R*$^{+/+}$.